

# $^{119}\text{Sn}$ -NMR spectroscopic study of the 1,3-dichloro- and 1,3-diacetoxytetra-*n*-butyldistannoxane binary system

Dennis L. Hasha \*

Department of Chemistry, University of Missouri-Rolla, Rolla, MO 65409, USA

Received 14 August 2000; received in revised form 24 October 2000

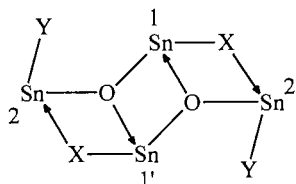
## Abstract

The binary  $[\text{Bu}_2\text{SnCl}]_2\text{O}/[\text{Bu}_2\text{SnOAc}]_2\text{O}$  ( $\text{OAc} = \text{O}_2\text{CCH}_3$ ) system is re-examined using  $^{119}\text{Sn}$ -NMR spectroscopy. Binary mixtures of  $[\text{Bu}_2\text{SnCl}]_2\text{O}$  and  $[\text{Bu}_2\text{SnOAc}]_2\text{O}$  reach equilibrium rapidly, producing all five possible mixed distannoxane dimers, differing in the ratio and relative positions of Cl and acetoxy ligands. The rapid formation of the product dimers results from the intermolecular exchange of the ligands one at a time. The  $^{119}\text{Sn}$ -NMR spectral data are consistent with time-averaged ladder structures arising from rapidly interconverting ladder pairs. The equilibrium concentrations of the binary mixtures indicate that positional ordering of the ligands exists in the mixed dimers. A reversible configurational rearrangement is also observed in which the ligands associated with the same exocyclic tin atom undergo mutual exchange via rotation about the oxygen–exocyclic tin bond. The  $^{119}\text{Sn}$  spectral data of the binary system leads to the unambiguous assignment of the tin resonances of  $\{[\text{Bu}_2\text{SnOAc}]_2\text{O}\}_2$ :  $\delta_{\text{exo}} = -216.1$  ppm,  $\delta_{\text{endo}} = -227.9$  ppm. © 2001 Elsevier Science B.V. All rights reserved.

**Keywords:** Distannoxane; NMR; Rearrangement; Redistribution; Tin

## 1. Introduction

The dimeric nature of tetraorganodistannoxanes in noncoordinating solvents has been well established [1–25]. Comparison of solution and solid-state  $^{119}\text{Sn}$ -NMR spectra confirms that the dimeric ladder structure, which the tetraorganodistannoxanes are known to adopt in the solid state [21–27], is retained in solution [19,20,24,25]. In the ladder structure the tin, oxygen and bridging X ligands are essentially coplanar.



Each tin possesses two pendent organic groups; however, for reasons of clarity these have been omitted. The two tin sites, which are designated endocyclic, Sn(1) and Sn(1'), and exocyclic, Sn(2) and Sn(2'), are both

pentacoordinate with distorted trigonal bipyramidal symmetries. Ladder structures have successfully accounted for the simple two-line  $^{119}\text{Sn}$ -NMR solution spectra of  $\{[\text{R}_2\text{SnX}]_2\text{O}\}_2$  [7c,12–15,17] and the centrosymmetric 2:2 (X:Y) mixed dimers  $\{[\text{X}^n\text{Bu}_2\text{SnOSn}^n\text{Bu}_2\text{Y}]_2\text{O}\}_2$  [13–15,17]. In addition, ladder structures have been used to interpret the 18  $^{119}\text{Sn}$  resonances reported for the equimolar mixture of  $[\text{Bu}_2\text{SnCl}]_2\text{O}$  and  $[\text{Bu}_2\text{SnOAc}]_2\text{O}$  ( $\text{OAc} = \text{O}_2\text{CCH}_3$ ) [15]. Using ladder structures, Gross [15] concluded that the equimolar mixture consisted of the reactant dimers  $\{[\text{Bu}_2\text{SnCl}]_2\text{O}\}_2$  and  $\{[\text{Bu}_2\text{SnOAc}]_2\text{O}\}_2$ , and four of five possible acetoxy-bridged mixed distannoxane dimers. The mixed dimers differ in the relative number and positions of the Cl and acetoxy ligands: one 3:1 (Cl:OAc) dimer, one 1:3 dimer and two 2:2 dimers. Jain et al. [17] identified similar F-bridged products in the binary mixtures of  $[\text{Bu}_2\text{SnF}]_2\text{O}/[\text{Bu}_2\text{Sn}(\text{O}_2\text{CR})]_2\text{O}$  ( $\text{R} = \text{CH}_3$ ,  $^i\text{Bu}$  and  $\text{Ph}$ ). In contrast, the equimolar  $[\text{Bu}_2\text{SnCl}]_2\text{O}/[\text{Bu}_2\text{SnBr}]_2\text{O}$  mixture is composed of a statistical distribution of the reactant dimers and all five possible Cl:Br mixed distannoxane dimers [20]. The NMR spectral data of the  $[\text{Bu}_2\text{SnCl}]_2\text{O}/[\text{Bu}_2\text{SnBr}]_2\text{O}$  binary system are consistent with time-averaged dimeric

\* Fax: +1-573-3416033.

E-mail address: dhasha@umr.edu (D.L. Hasha).

structures resulting from the intradimeric distannoxane process [19,21,23], i.e. rapidly interconverting ladder pairs. The discrepancy in the number of observed mixed distannoxane dimers led us to question the use of ladder structures to describe the room-temperature NMR spectral data of  $[^n\text{Bu}_2\text{SnCl}]_2\text{O}/[^n\text{Bu}_2\text{SnOAc}]_2\text{O}$  mixtures, and has prompted a reinvestigation of this binary system.

## 2. Experimental

The preparation of  $[^n\text{Bu}_2\text{SnCl}]_2\text{O}$  and  $[^n\text{Bu}_2\text{SnOAc}]_2\text{O}$  was conducted by literature methods [11,20]. Binary mixtures of  $[^n\text{Bu}_2\text{SnCl}]_2\text{O}$  and  $[^n\text{Bu}_2\text{SnOAc}]_2\text{O}$ , with approximate mole ratios 10:1, 3:1, 1:1, 1:3, 1:10 (Cl:OAc) were prepared by dissolving the appropriate amount of distannoxanes in 0.5 ml benzene- $d_6$ . The desired quantities of  $[^n\text{Bu}_2\text{SnCl}]_2\text{O}$  and  $[^n\text{Bu}_2\text{SnOAc}]_2\text{O}$  were determined by constraining the total tin concentration of each solution to  $[\text{Sn}]_{\text{T}} = 2.0 \text{ M}$ .

The 111.96 MHz and 149.08 MHz  $^{119}\text{Sn}$ -NMR spectra were acquired using Varian INOVA 300 and 400 NMR spectrometers respectively. The chemical shift scale of the spectrum was referenced to internal  $(\text{CH}_3)_4\text{Sn}$  (TMT). Quantification of the  $^{119}\text{Sn}$ -NMR spectra was ensured by using a recycle time of 1.5 s, which is substantially longer than the spin-lattice relaxation times observed: 40 to 100 ms (at 149.08 MHz). The  $^{119}\text{Sn}$  2D INADEQUATE experiment was optimized for  $J(^{119}\text{Sn}, ^{119}\text{Sn}) = 60 \text{ Hz}$ . Two-dimensional (2D)  $^{119}\text{Sn}$  chemical exchange (EXSY)

experiments were conducted at 328 K on the equimolar mixture. In order to extract exchange rates, the observed integrated intensities (volume) of the two-dimensional spectra were fit to the kinetic parameters of the rate matrix  $\mathbf{L}$ . The off-diagonal elements of the rate matrix  $L_{j,i}$  are given by the pseudo-first-order rate constants  $-K_{i \rightarrow j}$ , which provide the rate of magnetization transfer from site  $i$  to  $j$ . The 2D volume matrix  $\mathbf{I}$  is related to  $\mathbf{L}$  by

$$\mathbf{L} = \frac{\ln(\mathbf{P}^{-1}\mathbf{I})}{\tau_{\text{m}}} = \frac{\ln \mathbf{J}}{\tau_{\text{m}}},$$

where  $\mathbf{J}$  is the normalized volume matrix and  $\mathbf{P}$  is the volume matrix at  $\tau_{\text{m}} = 0$ . The elements of the diagonal matrix  $\mathbf{P}$  are proportional to the equilibrium populations. The off-diagonal elements of  $\mathbf{L}$  are the elements of  $\ln \mathbf{J}$  and are readily calculated via matrix diagonalization of  $\mathbf{J}$  [28–32]. The error in the reported rate constants are estimated to be  $\pm 15$ –25% relative.

## 3. Results and discussion

The  $[^n\text{Bu}_2\text{SnCl}]_2\text{O}/[^n\text{Bu}_2\text{SnOAc}]_2\text{O}$  binary system reaches equilibrium rapidly at room temperature. The 111.96 MHz  $^{119}\text{Sn}$ -NMR spectrum of a solution containing equimolar quantities of  $[^n\text{Bu}_2\text{SnCl}]_2\text{O}$  and  $[^n\text{Bu}_2\text{SnOAc}]_2\text{O}$ , with tin concentration  $[\text{Sn}]_{\text{T}} = 2.0 \text{ M}$ , consists of 20 resonances; see Fig. 1. This corresponds to the same number of distinct tin chemical environments detected in the  $^{119}\text{Sn}$ -NMR spectrum of the equimolar  $[^n\text{Bu}_2\text{SnCl}]_2\text{O}/[^n\text{Bu}_2\text{SnBr}]_2\text{O}$  mixture [20]. However, the  $^{119}\text{Sn}$ -NMR spectrum obtained by Gross of the equimolar  $[^n\text{Bu}_2\text{SnCl}]_2\text{O}/[^n\text{Bu}_2\text{SnOAc}]_2\text{O}$  binary mixture at half the tin concentration contains 19 resolved resonances, whereas only 18 resonances were reported [15]. The additional two resonances detected in the spectrum presented in Fig. 1 are located at  $-147.6$  and  $-221.3 \text{ ppm}$ . The high-frequency resonance,  $-147.6 \text{ ppm}$ , corresponds to the neglected resonance detected in the spectrum obtained by Gross [15], whereas the other resonance is only partially resolved at higher concentration. The four resonances due to the reactant dimers,  $\{[^n\text{Bu}_2\text{SnCl}]_2\text{O}\}_2$ , **4Cl**, ( $-90.0$  and  $-142.5 \text{ ppm}$ ) and  $\{[^n\text{Bu}_2\text{SnOAc}]_2\text{O}\}_2$ , **4OAc**, ( $-216.1$  and  $-227.9 \text{ ppm}$ ), are readily identified. The additional 16 resonances observed in the equimolar mixture are due to mixed distannoxane dimers resulting from the redistribution of the Cl and acetoxy ligands. By varying the concentration of the reactants, the eight resonances assigned to the 3:1 (Cl:OAc), **I**, and 1:3, **II**, distannoxane dimers by Gross [15] are confirmed. The  $^{119}\text{Sn}$  2D INADEQUATE spectrum of the equimolar mixture, shown in Fig. 2, reveals that

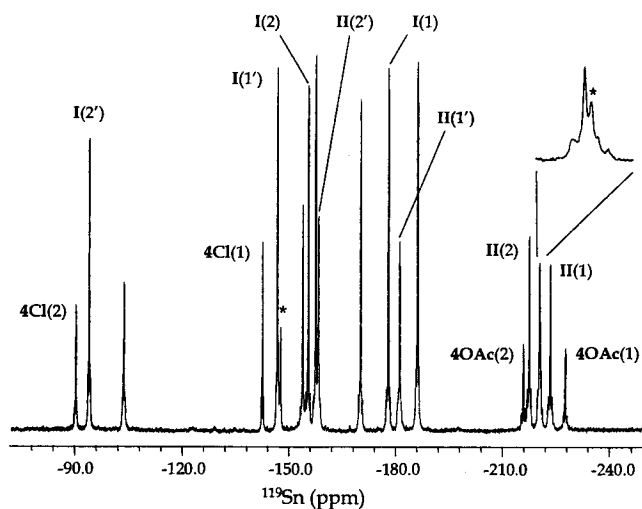


Fig. 1. 111.96 MHz  $^{119}\text{Sn}$ -NMR spectrum of the equimolar  $[^n\text{Bu}_2\text{SnCl}]_2\text{O}/[^n\text{Bu}_2\text{SnOAc}]_2\text{O}$  mixture with  $[\text{Sn}]_{\text{T}} = 2.0 \text{ M}$  in benzene- $d_6$  at 298 K. The resonances denoted with asterisks are the unreported resonances of Gross [15]; see text.

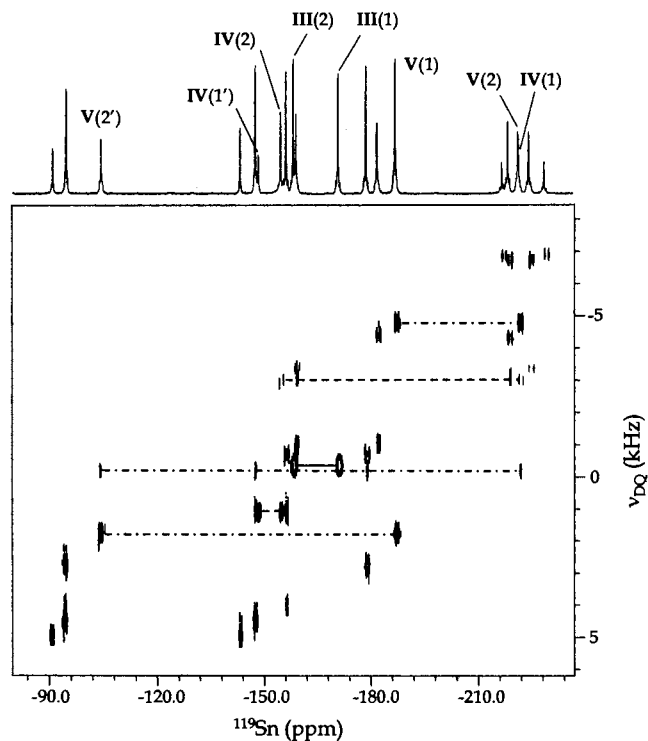
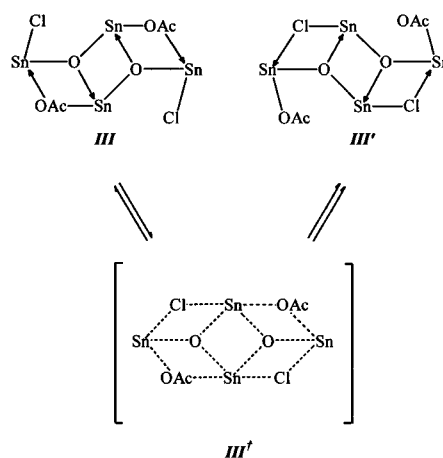


Fig. 2. 111.96 MHz  $^{119}\text{Sn}$  2D INADEQUATE spectrum of the equimolar  $[\text{Bu}_2\text{SnCl}]_2\text{O}/[\text{Bu}_2\text{SnOAc}]_2\text{O}$  mixture with  $[\text{Sn}]_{\text{T}} = 2.0$  M in benzene- $d_6$  at 298 K. The experiment was optimized for 60 Hz couplings,  $\tau_{\text{DQ}} = 4.17$  ms. Lines are drawn to show the coupling network associated with the 2:2 mixed distannoxane dimers: **III** (—), **IV** (---) and **V** (- · - · -).

the remaining eight resonances are due to three 2:2 mixed distannoxane dimers: **III**,  $-157.6(1)$  and  $-170.1(1)$  ppm; **IV**,  $-147.6(1)$ ,  $-153.9(2)$  and  $-221.0(1)$  ppm; **V**,  $-103.4(1)$ ,  $-186.4(2)$  and  $-220.7(1)$  ppm. The numbers in parentheses are the relative numbers of tin nuclei responsible for each resonance. The number of 2:2 mixed dimer resonances and their distribution is the same as observed for the 2:2 mixed dimers of the  $[\text{Bu}_2\text{SnCl}]_2\text{O}/[\text{Bu}_2\text{SnBr}]_2\text{O}$  binary system. This observation indicates that the  $^{119}\text{Sn}$ -NMR spectra of the  $[\text{Bu}_2\text{SnCl}]_2\text{O}/[\text{Bu}_2\text{SnOAc}]_2\text{O}$  binary system are consistent with time-averaged ladder structures, resulting from rapidly interconverting ladder pairs (intradimeric distannoxane process); Scheme 1. The symmetric transition state, **III**<sup>†</sup>, is characterized by ligands located at positions that are weighted averages of the bridging and nonbridging sites of the ladder structures, **III** and **III**'. Owing to the higher donor power of the carbonyl oxygen compared with Cl, the acetoxy ligand is anticipated to preferentially occupy the bridging sites [18,24]. Although, the higher affinity of the acetoxy ligand for the bridging sites dictates that the equilibrium shifts in favor of **III**, this equilibrium shift is expected to be slight, since the equimolar mixture con-

tains all possible distannoxane dimers. Pictorial representations of the time-averaged structures are presented in Fig. 3.

Spectral assignments of the  $^{119}\text{Sn}$ -NMR spectra for the binary  $[\text{Bu}_2\text{SnCl}]_2\text{O}/[\text{Bu}_2\text{SnOAc}]_2\text{O}$  mixtures are achieved using time-averaged ladder structures, coupled with the unambiguous assignments of the reactants. Otera et al. [13] assigned the high-frequency resonance of **4Cl** to the exocyclic environment based on the relative number of Cl ligands attached to the endo- and exocyclic tin atoms. However, the assignment of the  $^{119}\text{Sn}$ -NMR spectrum of **4OAc** has been debated ever since the low-frequency resonance was tentatively attributed to the exocyclic tin atoms [14]. This assignment was subsequently reversed by Gross [15] without comment. Chemical shift comparisons with the 1-alkoxy-3-acetoxytetra-*n*-butyldistannoxanes and arguments based on a suspected enhancement in shielding upon replacement of an oxygen in the endocyclic fragment,  $\text{SnO}_2(\text{OAc})$ , with an acetoxy ligand led Michel and coworkers [18,19] to conclude that the original assignment is correct:  $\delta_{\text{endo}} > \delta_{\text{exo}}$ . Recently, unambiguous, yet contradictory, tin assignments for  $\{[(\text{CH}_3)_2\text{SnOAc}]_2\text{O}\}_2$  ( $\delta_{\text{exo}} = -173.8$  ppm,  $\delta_{\text{endo}} = -190.2$  ppm) and  $\{[(\text{CH}_3)_2\text{Sn}(\text{O}_2\text{C}^i\text{Bu})]_2\text{O}\}_2$  ( $\delta_{\text{endo}} = -188.2$  ppm,  $\delta_{\text{exo}} = -195.1$  ppm) have been determined using the  $^1\text{H}\{-^{119}\text{Sn}\}$  gradient-enhanced HMQC experiment [25]. For **4OAc**, coincidental chemical shifts of the  $\alpha$ -methylene protons prevent the  $^1\text{H}\{-^{119}\text{Sn}\}$  gradient-enhanced HMQC experiment from differentiating the desired long-range  $^1\text{H}\{-^{119}\text{Sn}\}$  correlations. Fortunately, the NMR spectral data of the binary mixtures permits unambiguous tin assignments for **4OAc**. The  $^{119}\text{Sn}$  2D INADEQUATE spectrum segregates the tin resonances for a given distannoxane dimer into two groups (endo- and exocyclic) without identifying the group to which



Scheme 1.

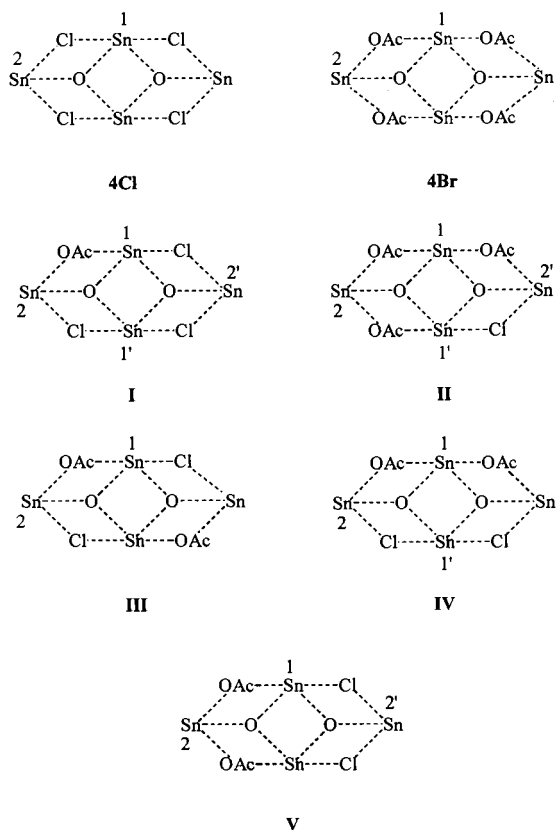


Fig. 3. Pictorial representation of the time-averaged dimeric distannoxane structures resulting from the intradimeric distannoxane process, i.e. rapid interconverting ladder structures (Scheme 1).

the resonance belongs. The endo- or exocyclic identity of the resonances is determined using the  $^{119}\text{Sn}$  EXSY spectrum of the equimolar mixture at 328 K. The  $^{119}\text{Sn}$  EXSY spectrum contains crosspeaks due to the intermolecular redistribution of the ligands, as well as an intramolecular fluxional process (oxygen–exocyclic tin bond rotation); see Fig. 4. Crosspeaks connecting the endo- and exocyclic tin resonances of the reactant dimers,  $4\text{Cl}(1) \leftrightarrow 4\text{Cl}(2)$  and  $4\text{OAc}(1) \leftrightarrow 4\text{OAc}(2)$ , are not detected. Similarly, crosspeaks between the endo- and exocyclic tin atoms of the mixed dimers are also absent; for example,  $\text{I}(1) \leftrightarrow \text{I}(2)$ . Therefore, endo- and exocyclic tin exchange does not occur, confirming that the integrity of the tin sites is maintained during the mixing time (20 ms) of the EXSY experiment. Intense intermolecular crosspeaks are present for the following distannoxane dimer pairs:  $\text{I} \leftrightarrow \text{V}$ ,  $\text{II} \leftrightarrow \text{III}$ ,  $\text{II} \leftrightarrow \text{IV}$ ,  $\text{III} \leftrightarrow \text{IV}$  and  $\text{II} \leftrightarrow 4\text{OAc}$ . Weaker intermolecular crosspeaks are observed for  $4\text{Cl} \leftrightarrow \text{I}$ ,  $\text{I} \leftrightarrow \text{III}$ ,  $\text{I} \leftrightarrow \text{IV}$  and  $\text{II} \leftrightarrow \text{V}$ . In addition, numerous very weak crosspeaks, which arise from two-step exchanges, are also detected. Excluding the crosspeaks due to the interconversion of **III** and **IV**, the major intermolecular crosspeaks are consistent with the replacement of the ligands one at a time. Thus, by mapping out the intermolecular ex-

change crosspeak network a connection from the tin resonances of **4Cl** to the corresponding peaks of **4OAc** is achieved. Starting with the exocyclic tin resonance of **4Cl**, crosspeaks are observed connecting **4Cl**(2) to **I**(2) and **I**(2'), ( $-89.7$ ,  $-93.6$ ) and ( $-89.7$ ,  $-146.0$ ). The exocyclic tin atoms of **I** also exhibit exchange crosspeaks to **V**(2), ( $-93.6$ ,  $-102.9$ ) and ( $-146.0$ ,  $-219.4$ ), which in turn possesses exchange crosspeaks to **II**(2) and **II**(2'), ( $-102.9$ ,  $-157.3$ ) and ( $-219.4$ ,  $-216.4$ ). Both exocyclic tin atoms of **II** exhibit crosspeaks to the high-frequency resonance of **4OAc**, identifying the resonance located at  $-214.3$  ppm as the exocyclic tin atom (see Fig. 4). If the starting point is chosen to be the endocyclic tin resonance of **4Cl** the same conclusion is reached.

Assignment of the tin resonances for the 3:1 mixed distannoxane dimer, **I**, is accomplished by comparison with **4Cl**. The Sn(2') environment of **I**, which is similar to the exocyclic tin of **4Cl**, is assigned to the resonance observed at  $-93.9$  ppm. The endocyclic tin atoms of **I**, which are identified by examination of the  $^{119}\text{Sn}$  2D INADEQUATE and EXSY spectra, are assigned to the two resonances at  $-146.8$  and  $-178.1$  ppm. Since **I**(1') closely approximates the endocyclic tin environment of **4Cl**, it is assigned to the high-frequency resonance,  $-146.8$  ppm. It follows that the remaining two tin atoms, **I**(2) and **I**(1), are assigned to  $-155.5$  ppm and  $-178.1$  ppm respectively. Similarly, comparison of **II** and **4OAc**, coupled with the  $^{119}\text{Sn}$  2D INADEQUATE and EXSY spectra, yields the tin assignments for the 1:3 mixed distannoxane dimer. Using the chemical shift differences observed between **I** and **II**, the resonances of the 2:2 mixed distannoxane dimers are readily assigned; see Table 1.

In the  $^{119}\text{Sn}$  EXSY spectrum of the  $[\text{Bu}_2\text{SnCl}]_2\text{O}/[\text{Bu}_2\text{SnOAc}]_2\text{O}$  equimolar mixture the intermolecular exchange crosspeaks are observed at significantly shorter mixing times ( $\tau_m \approx 20$  ms) than the  $^{13}\text{C}$  EXSY crosspeaks of the corresponding  $[\text{Bu}_2\text{SnCl}]_2\text{O}/[\text{Bu}_2\text{SnBr}]_2\text{O}$  solution ( $\tau_m \approx 500$  ms) [20]. This observation indicates that the  $[\text{Bu}_2\text{SnCl}]_2\text{O}/[\text{Bu}_2\text{SnOAc}]_2\text{O}$  binary system undergoes ligand redistribution at a faster rate and reaches equilibrium more quickly than the  $[\text{Bu}_2\text{SnCl}]_2\text{O}/[\text{Bu}_2\text{SnBr}]_2\text{O}$  system. The unidirectional pseudo-first-order rate constants  $K_{A \rightarrow B}$  and rates of exchange  $K_{A \rightarrow B}[A]$  extracted from the  $^{119}\text{Sn}$  EXSY spectra reveal differential exchange characteristics in this system; see Table 2. The rate constants suggest an exocyclic acetoxy ligand effect, in which the acetoxy ligand facilitates the exchange of its exocyclic partner relative to Cl. For example, the acetoxy ligands of **III** and **IV** improve the leaving ability of the Cl ligands, preferentially converting both **III** and **IV** into **II**:  $K_{\text{III} \rightarrow \text{II}} \approx K_{\text{IV} \rightarrow \text{II}} > K_{\text{III} \rightarrow \text{I}} \approx K_{\text{IV} \rightarrow \text{I}}$ . Likewise, the acetoxy ligands of **V**, which are attached to the same exocyclic tin, mutually accentuate each other's leaving ability, prefer-

entially producing **I** from **V**,  $K_{V \rightarrow I} > K_{V \rightarrow II}$ . The ligand exchange mechanism for the  $[^n\text{Bu}_2\text{SnCl}]_2\text{O}/[^n\text{Bu}_2\text{SnOAc}]_2\text{O}$  system is left undetermined; however, it is anticipated to be the four-centered transition state mechanism, which has been shown to be responsible for the ligand exchange among Cl:Br mixed distannoxanes [20].

The intramolecular exchange crosspeaks of the  $^{119}\text{Sn}$  EXSY spectrum result from the mutual exchange of the endocyclic tin atoms of **I** and **II**,  $\text{I}(1) \leftrightarrow \text{I}(1')$  and  $\text{II}(1) \leftrightarrow \text{II}(1')$ , as well as the interconversion of rotational isomers **III** and **IV**,  $\text{IV}(1) \leftrightarrow \text{III}(1) \leftrightarrow \text{IV}(1')$  and  $\text{III}(2) \leftrightarrow \text{IV}(2)$ . This intramolecular process occurs via rotation of the oxygen–exocyclic tin bond; Scheme 2.

Oxygen–exocyclic tin bond rotation, which has also been observed for Cl:Br mixed distannoxane dimers [20], is the reversible analog to the configurational rearrangement proposed by Michel and coworkers [19]. The rate constants determined from the  $^{119}\text{Sn}$  EXSY experiment for the endocyclic tin atoms of **I** and **II** are equal to the rate of bond rotation about the oxygen–exocyclic tin bond. Rotation of either oxygen–exocyclic tin bond results in the interconversion of **III** and **IV**, which leads to an intramolecular exchange rate constant that is twice the rate of the oxygen–exocyclic tin bond rotation. At 328 K the bond rotation rates are  $k(\text{I}) = 1.06 \text{ s}^{-1}$ ,  $k(\text{II}) = 10.1 \text{ s}^{-1}$ ,  $k(\text{III}) = 4.76 \text{ s}^{-1}$  and  $k(\text{IV}) = 5.65 \text{ s}^{-1}$ . These rates are significantly slower

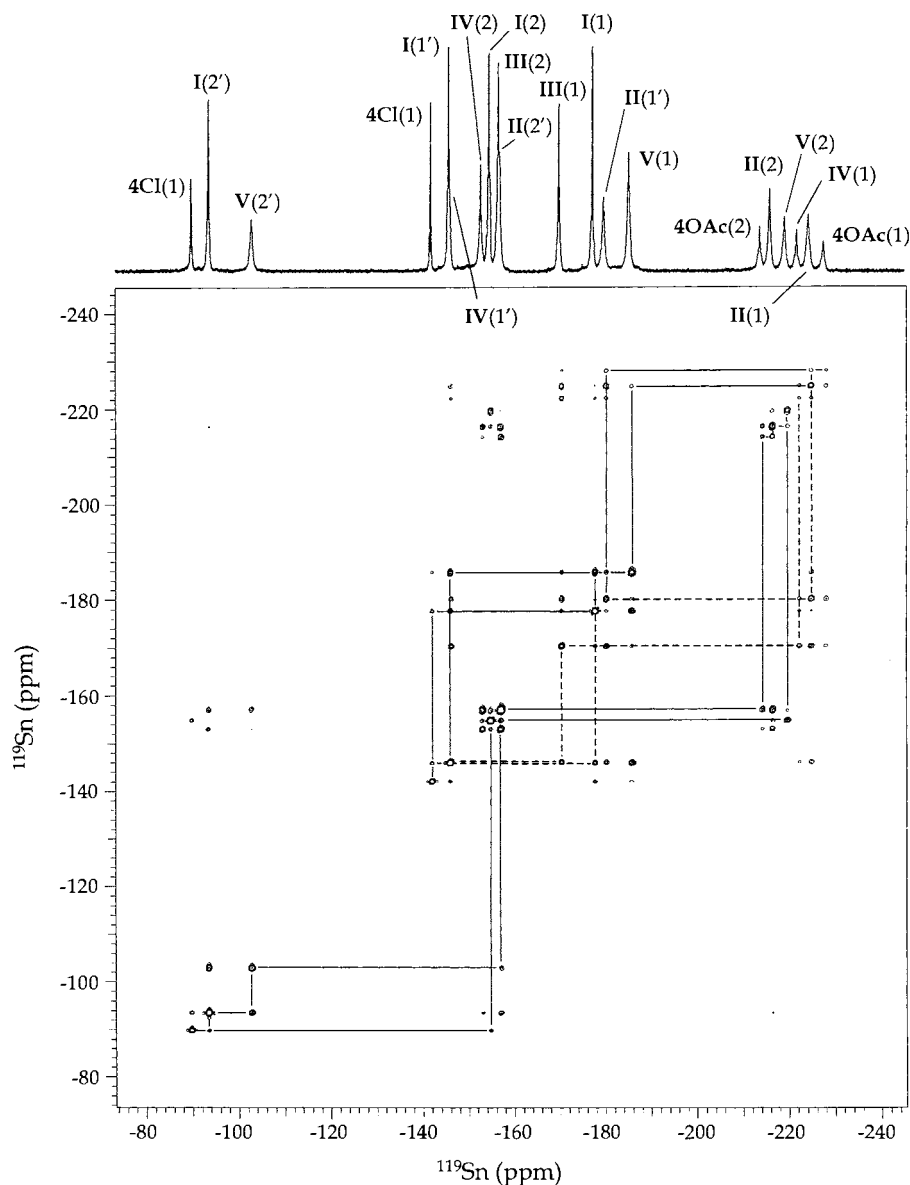


Fig. 4. 149.08 MHz  $^{119}\text{Sn}$  EXSY spectrum of the equimolar  $[^n\text{Bu}_2\text{SnCl}]_2\text{O}/[^n\text{Bu}_2\text{SnOAc}]_2\text{O}$  mixture with  $[\text{Sn}]_{\text{T}} = 2.0 \text{ M}$  in benzene- $d_6$  at 328 K. Mixing time is set to 20 ms. Solid lines map out one of the intermolecular exchange pathways linking the resonances of **4Cl** and **4OAc**. Dashed lines connect crosspeaks arising from the rotation of the oxygen–exocyclic tin bond.

Table 1

$^{119}\text{Sn}$ -NMR spectral assignments of distannoxane dimers present in  $[\text{Bu}_2\text{SnCl}]_2\text{O}/[\text{Bu}_2\text{SnOAc}]_2\text{O}$  binary mixtures

Dimer <sup>a</sup>	$^{119}\text{Sn}$ ( $\delta$ ppm) <sup>b</sup>			
	Sn(1)	Sn(1')	Sn(2)	Sn(2')
<b>4Cl</b>	-142.5	(-142.5) <sup>c</sup>	-90.0	(-90.0)
<b>4OAc</b>	-227.9	(-227.9)	-216.1	(-216.1)
<b>I</b>	-178.1	-146.8	-155.5	-93.8
<b>II</b>	-223.7	-181.2	-217.8	-158.3
<b>III</b>	-170.1	(-170.1)	-157.6	(-157.6)
<b>IV</b>	-221.0	-147.6	-153.9	(-153.9)
<b>V</b>	-186.4	(-186.4)	-220.7	-103.4

<sup>a</sup> The time-averaged structures and the numbering scheme are shown in Fig. 3.

<sup>b</sup> The chemical shift scale is referenced using an internal shift standard, TMT = 0.0 ppm. The shifts are reported for the equimolar  $[\text{Bu}_2\text{SnCl}]_2\text{O}/[\text{Bu}_2\text{SnOAc}]_2\text{O}$  mixture in benzene- $d_6$  with  $[\text{Sn}]_{\text{T}} = 2.0$  M at 298 K. Variations in the chemical shifts due to composition are less than 0.02 ppm.

<sup>c</sup> Chemical shifts in parentheses are due to symmetry-related environments.

than the bond rotation rates observed for the Cl:Br mixed dimers of ca.  $26\text{ s}^{-1}$  [20], indicating that the bulkier acetoxy ligands sterically hinder oxygen–exocyclic tin bond rotation. As the number of the acetoxy groups in the Cl:OAc dimers increases, the rate of bond rotation also increases. This behavior suggests that, relative to Cl, the nonbridging acetoxy ligand interacts with the proximal endocyclic tin atom sufficiently to weaken the ligand–endocyclic tin bond, thus facilitating rotation about the distal oxygen–exocyclic tin bond.

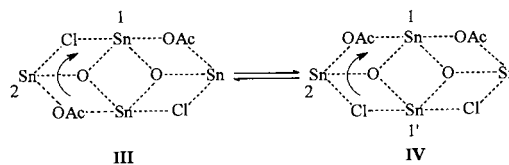
The compositions of the binary mixtures, obtained by integration of the  $^{119}\text{Sn}$ -NMR spectra, are given in Table 3. The equilibrium concentrations of **4Cl**, **4OAc**, **I** and **II**, as well as the sum of the 2:2 mixed dimers, are satisfactorily represented by a statistical distribution. However, a random distribution cannot account for the observation that the concentrations of the 2:2 mixed dimers are not equal. At all compositions the most

Table 2

The unidirectional pseudo-first-order rates constants and exchange rates for ligand exchange in the equimolar  $[\text{Bu}_2\text{SnCl}]_2\text{O}/[\text{Bu}_2\text{SnOAc}]_2\text{O}$  mixture in benzene- $d_6$  at 328 K and  $[\text{Sn}]_{\text{T}} = 2.0$  M

Species		Pseudo-first-order rate constants ( $\text{s}^{-1}$ ) <sup>a</sup>		Exchange rates ( $\text{mol dm}^{-3} \text{s}^{-1}$ )	
A	B	$K_{\text{A} \rightarrow \text{B}}$	$K_{\text{B} \rightarrow \text{A}}$	$K_{\text{A} \rightarrow \text{B}}[\text{A}]$	$K_{\text{B} \rightarrow \text{A}}[\text{B}]$
<b>4Cl</b>	<b>I</b>	1.53	0.31	$4.1 \times 10^{-2}$	$3.9 \times 10^{-2}$
<b>I</b>	<b>III</b>	0.48	0.92	$6.1 \times 10^{-2}$	$6.0 \times 10^{-2}$
<b>I</b>	<b>IV</b>	0.44	1.03	$5.6 \times 10^{-2}$	$6.4 \times 10^{-2}$
<b>I</b>	<b>V</b>	4.20	6.91	$53.3 \times 10^{-2}$	$60.8 \times 10^{-2}$
<b>II</b>	<b>III</b>	2.27	3.46	$25.7 \times 10^{-2}$	$22.7 \times 10^{-2}$
<b>II</b>	<b>IV</b>	1.54	3.30	$17.4 \times 10^{-2}$	$20.6 \times 10^{-2}$
<b>II</b>	<b>V</b>	0.65	0.90	$7.3 \times 10^{-2}$	$7.9 \times 10^{-2}$
<b>4OAc</b>	<b>II</b>	7.02	1.47	$17.6 \times 10^{-2}$	$16.6 \times 10^{-2}$

<sup>a</sup> Errors estimated to be  $\pm 15$ –25%.



Scheme 2.

abundant 2:2 mixed dimer is **V**,  $[\text{V}] > [\text{III}] > [\text{IV}]$ . If the positional ordering of the ligands is determined by preferential occupation of the bridging sites by either ligand, the most abundant 2:2 mixed dimer is expected to be **III**. These results suggest that any preference for the bridging sites exhibited by either ligand is overwhelmed by a not yet understood special stability associated with the acetoxy ligands bound to the same exocyclic tin atom.

#### 4. Conclusion

Binary mixtures containing  $[\text{Bu}_2\text{SnCl}]_2\text{O}$  and  $[\text{Bu}_2\text{SnOAc}]_2\text{O}$  in benzene- $d_6$  are composed of the reactant dimers and all possible Cl:OAc mixed distannoxane dimers. The  $^{119}\text{Sn}$ -NMR spectral data are consistent with time-averaged ladder structures resulting from the intradimeric distannoxane process; i.e. interconverting ladder structures. The observed concentrations of the distannoxane dimers in the binary mixtures are not described by a random distribution. The relative concentrations of the 2:2 mixed dimers suggest that acetoxy ligands prefer to be bound to the same exocyclic tin atom. The rapid formation of the mixed distannoxane dimers occurs via an intermolecular exchange process in which the ligands are replaced one at a time. Differential exchange rates are observed, suggesting that the acetoxy ligand improves the leaving ability of its exocyclic partner. In addition, a reversible oxygen–exocyclic tin bond rotation is detected in the mixed distannoxanes **I**, **II**, **III** and **IV**. Finally, unam-

Table 3

Composition of  $[{}^n\text{Bu}_2\text{SnCl}]_2\text{O}/[{}^n\text{Bu}_2\text{SnOAc}]_2\text{O}$  mixtures<sup>a</sup>

Cl:OAc mixture <sup>b</sup>	Mole fraction <sup>c</sup>								
	$X_{\text{Cl}}^0$ <sup>d</sup>	$X_{4\text{Cl}}$	$X_{4\text{OAc}}$	$X_{\text{I}}$	$X_{\text{II}}$	$X_{\text{III}}$	$X_{\text{IV}}$	$X_{\text{V}}$	$X_{\text{Cl}}^{\text{T}}/4$ <sup>e</sup>
10:1	0.920	0.700	nd <sup>f</sup>	0.270	nd	0.010	0.005	0.015	0.918
3:1	0.753	0.314	0.003	0.441	0.037	0.066	0.042	0.096	0.756
1:1	0.506	0.047	0.049	0.250	0.233	0.133	0.101	0.187	0.503
1:3	0.250	0.001	0.297	0.039	0.433	0.071	0.055	0.105	0.253
1:10	0.091	nd	0.683	0.002	0.277	0.013	0.008	0.018	0.090

<sup>a</sup> Total tin concentration,  $[\text{Sn}]_{\text{T}} = 2.0 \text{ M}$ ; 1 mmol of tin in 0.5 ml benzene- $d_6$  at 298 K.<sup>b</sup> Actual initial composition in terms of mole ratio; Cl:OAc =  $[{}^n\text{Bu}_2\text{SnCl}]_2\text{O}:[{}^n\text{Bu}_2\text{SnOAc}]_2\text{O}$ .<sup>c</sup> Concentrations are obtained from integration of the  ${}^{119}\text{Sn}$ -NMR spectra acquired under quantitative conditions.<sup>d</sup>  $X_{\text{Cl}}^0$  is the initial concentration (mole fraction) of  $[{}^n\text{Bu}_2\text{SnCl}]_2\text{O}$ .<sup>e</sup>  $X_{\text{Cl}}^{\text{T}}/4 = X_{4\text{Cl}} + 0.75X_{\text{I}} + 0.25X_{\text{II}} + 0.5(X_{\text{III}} + X_{\text{IV}} + X_{\text{V}})$ .<sup>f</sup> Not detected.

ambiguous assignment of the  ${}^{119}\text{Sn}$ -NMR spectrum of  $\{[{}^n\text{Bu}_2\text{SnOAc}]_2\text{O}\}_2$  is achieved, attributing the high-frequency resonance to the exocyclic tin atom.

## References

- [1] R. Okawara, Proc. Chem. Soc. (1961) 383.
- [2] D.L. Alleston, A.G. Davies, B.N. Figgis, Proc. Chem. Soc. (1961) 457.
- [3] R. Okawara, M. Wada, J. Organomet. Chem. 1 (1963) 81.
- [4] W.J. Considine, J.J. Ventura, J. Org. Chem. 28 (1963) 221.
- [5] W.J. Considine, J.J. Ventura, A.J. Gibbons, Jr, A. Ross, Can. J. Chem. 41 (1963) 1239.
- [6] D.L. Alleston, A.G. Davies, M. Hancock, R.F.M. White, J. Chem. Soc. (1963) 5469.
- [7] D.L. Alleston, A.G. Davies, M. Hancock, J. Chem. Soc. (1964) 5744.
- [8] M. Wada, N. Nishino, R. Okawara, J. Organomet. Chem. 3 (1965) 1342.
- [9] R. Okawara, K. Yasuda, J. Organomet. Chem. 1 (1963) 356.
- [10] M. Wada, R. Okawara, J. Organomet. Chem. 8 (1967) 261.
- [11] Y. Maeda, R. Okawara, J. Organomet. Chem. 10 (1967) 247.
- [12] A.G. Davies, L. Smith, P.J. Smith, W. McFarlane, J. Organomet. Chem. 29 (1971) 245.
- [13] J. Otera, T. Yano, K. Nakashima, R. Okawara, Chem. Lett. (1984) 2109.
- [14] T. Yano, K. Nakashima, J. Otera, R. Okawara, Organometallics 4 (1985) 1501.
- [15] D. Gross, Inorg. Chem. 28 (1989) 2355.
- [16] V.B. Mikol, V.K. Jain, J. Organomet. Chem. 441 (1992) 215.
- [17] V.K. Jain, V.B. Mokal, P. Sandor, Magn. Reson. Chem. 30 (1992) 1158.
- [18] J. Bonetti, C. Gondard, R. Petiaud, M.F. Lauro, A. Michel, J. Organomet. Chem. 481 (1994) 7.
- [19] O. Primel, M.F. Llauro, R. Petiaud, A. Michel, J. Organomet. Chem. 558 (1998) 19.
- [20] D.L. Tierney, P.J. Moehs, D.L. Hasha, J. Organomet. Chem. in press.
- [21] C. Vasta, V.K. Jain, T. Kesavadas, E.R.T. Tiekink, J. Organomet. Chem. 408 (1991) 157.
- [22] C. Vasta, V.K. Jain, T.K. Das, E.R.T. Tiekink, J. Organomet. Chem. 418 (1991) 329.
- [23] E.R.T. Tiekink, M. Gielen, A. Bouhid, M. Biesemans, R. Willem, J. Organomet. Chem. 494 (1995) 247.
- [24] D. Daternieks, K. Jurkschat, S. van Dreumel, E.R.T. Tiekink, Inorg. Chem. 36 (1997) 2023.
- [25] F. Ribot, C. Sanchez, A. Meddour, M. Gielen, E.R.T. Tiekink, M. Biesemans, R. Willem, J. Organomet. Chem. 552 (1998) 177.
- [26] (a) R. Okwara, N. Kasai, K. Yasuda, 2nd International Symposium on Organometallic Chemistry, Wisconsin, 1965, p. 128. (b) Y.M. Chow, Inorg. Chem. 10 (1971) 673. (c) H. Matsuda, F. Mori, A. Kashiwa, S. Matsuda, N. Kasai, K. Jitsumori, J. Organomet. Chem. 34 (1972) 341. (d) C.D. Garner, B. Hughes, Inorg. Nucl. Chem. Lett. 12 (1976) 859. (e) R. Graziani, G. Bombieri, E. Forsellini, P. Furlan, V. Peruzzo, G. Tagliavini, J. Organomet. Chem. 125 (1977) 43. (f) R. Faggiani, J.P. Johnson, I.D. Brown, T. Birchall, Acta Crystallogr. Sect. B 34 (1978) 3743. (g) P.G. Harrison, M.J. Begley, K.C. Molloy, J. Organomet. Chem. 186 (1980) 213. (h) H. Puff, E. Friedrichs, F. Visel, Z. Anorg. Allg. Chem. 477 (1981) 50. (i) R. Graziani, U. Castellato, G. Plazzonga, Acta Crystallogr. Sect. C 39 (1983) 1188. (j) H. Puff, I. Bung, E. Friedrichs, A. Jansen, J. Organomet. Chem. 254 (1983) 23. (k) J.F. Vollano, R.O. Day, R.R. Holmes, Organometallics 3(1984) 745. (l) D. Dakternieks, R.W. Gable, B.F. Hoskins, Inorg. Chim. Acta 85 (1984) L43. (m) V. Chandrasekhar, R.O. Day, J.M. Holmes, R.R. Holmes, Inorg. Chem. 27 (1988) 958. (n) S.P. Narula, S.K. Bharadwaj, H.K. Sharma, G. Maires, P. Barbier, G. Nowogrocki, J. Chem. Soc. Dalton Trans. (1988) 1719. (o) G.K. Sandhu, N. Sharma, E.R.T. Tiekink, J. Organomet. Chem. 371 (1989) C1. (p) C.S. Parulekar, V.K. Jain, T.K. Das, A.R. Gupta, B.F. Hoskins, E.R.T. Tiekink, J. Organomet. Chem. 372 (1989) 193. (q) N.A. Alcock, S.M. Roe, J. Chem. Soc. Dalton Trans. (1989) 1589. (r) E.R.T. Tiekink, Appl. Organomet. Chem. 5 (1991) 1. (s) M. Bouâlam, R. Willem, M. Biesemans, B. Mahieu, J. Meunier-Piret, M. Gielen, Main Group Met. Chem. 14 (1991) 41. (t) M. Gielen, J. Meunier-Piret, M. Biesemans, R. Willem, A. El Khoulfi, Appl. Organomet. Chem. 6 (1992) 59. (u) M. Gielen, A. El Khoulfi, M. Biesemans, R. Willem, Polyhedron 11 (1992) 1861. (v) M. Gielen, M. Biesemans, A. El Khoulfi, J. Meunier-Piret, F. Kayser, R. Willem, J. Fluorine Chem. 64 (1993) 279. (w) M. Gielen, A. Bouhid, R. Willem, V.I. Bregadze, L.V. Ermanson, E.R.T. Tiekink, J. Organomet. Chem. 501, (1995) 277. (x) M. Gielen, E.R.T. Tiekink, A. Bouhid, D. de Vos, M. Biesemans, I. Verbruggen, R. Willem, Appl. Organomet. Chem. 9 (1995) 639.
- [27] T.P. Lockhart, W.F. Manders, E.M. Holt, J. Am. Chem. Soc. 108 (1986) 6611.
- [28] C.L. Perrin, R.K. Gipe, J. Am. Chem. Soc. 106 (1984) 4036.
- [29] J.W. Keepers, T.L. James, J. Magn. Reson. 57 (1984) 404.
- [30] J. Bremer, G.L. Mendz, W.J. Moore, J. Am. Chem. Soc. 106 (1984) 4691.
- [31] E.T. Olejniczak, R.T. Gampe, Jr, S.W. Fesik, J. Magn. Reson. 67 (1986) 28.
- [32] C.L. Perrin, T.J. Dwyer, Chem. Rev. 90 (1990) 935.